catalysts

MDPI

Article

Synthesis, Characterizations and Catalysis of Sulfated Silica and Nickel Modified Silica Catalysts for Diethyl Ether (DEE) Production from Ethanol towards Renewable Energy Applications

Karna Wijaya [1,*,†], Melynatri Laura Lammaduma Malau [1], Maisari Utami [2], Sri Mulijani [3], Aep Patah [4], Arief Cahyo Wibowo [5], Murugesan Chandrasekaran [6], Jothi Ramalingam Rajabathar [7,*,†] and Hamad A. Al-Lohedan [7]

1 Department of Chemistry, Faculty of Mathematics and Natural Sciences, Universitas Gadjah Mada, Yogyakarta 55281, Indonesia; melynatrilaura@mail.ugm.ac.id
2 Department of Chemistry, Faculty of Mathematics and Natural Sciences, Universitas Islam Indonesia, Yogyakarta 55584, Indonesia; maisariutami@uii.ac.id
3 Department of Chemistry, Faculty of Mathematics and Natural Sciences, Institut Pertanian Bogor, Bogor 16680, Indonesia; srimulijani@apps.ipb.ac.id
4 Department of Chemistry, Faculty of Mathematics and Natural Sciences, Institut Teknologi Bandung, Bandung 40132, Indonesia; aep@chem.itb.ac.id
5 Department of Applied Sciences, College of Arts and Sciences, Abu Dhabi University, Abu Dhabi 59911, United Arab Emirates; arief.wibowo@adu.ac.ae
6 Department of Food Science and Biotechnology, Sejong University, Seoul 05006, Korea; chandrubdubio@gmail.com
7 Department of Chemistry, College of Science, King Saud University, P.O. Box 2455, Riyadh 11451, Saudi Arabia; hlohedan@ksu.edu.sa
* Correspondence: karnawijaya@ugm.ac.id (K.W.); rjothiram@gmail.com (J.R.R.)
† These two authors contributed equal.

check for updates

Citation: Wijaya, K.; Lammaduma Malau, M.L.; Utami, M.; Mulijani, S.; Patah, A.; Wibowo, A.C.; Chandrasekaran, M.; Rajabathar, J.R.; Al-Lohedan, H.A. Synthesis, Characterizations and Catalysis of Sulfated Silica and Nickel Modified Silica Catalysts for Diethyl Ether (DEE) Production from Ethanol towards Renewable Energy Applications. *Catalysts* **2021**, *11*, 1511. https://doi.org/10.3390/catal11121511

Academic Editors: Sekar Karthikeyan and Boopathy Ramasamy

Received: 16 November 2021
Accepted: 8 December 2021
Published: 11 December 2021

Publisher's Note: MDPI stays neutral with regard to jurisdictional claims in published maps and institutional affiliations.

Copyright: © 2021 by the authors. Licensee MDPI, Basel, Switzerland. This article is an open access article distributed under the terms and conditions of the Creative Commons Attribution (CC BY) license (https://creativecommons.org/licenses/by/4.0/).

Abstract: Sulfated silica (SO_4/SiO_2) and nickel impregnated sulfated silica ($Ni\text{-}SO_4/SiO_2$) catalysts have been successfully carried out for the conversion of ethanol into diethyl ether (DEE) as a biofuel. The aims of this research were to study the effects of acidity on the SO_4/SiO_2 and $Ni\text{-}SO_4/SiO_2$ catalysts in the conversion of ethanol into diethyl ether. This study focuses on the increases in activity and selectivity of SiO_2 with the impregnation of sulfate and Ni metal, which had good activity and acidity and were less expensive. The SO_4/SiO_2 catalysts were prepared using TEOS (Tetraethyl Orthosilicate) as a precursor and sulfuric acid with various concentrations (1, 2, 3, 4 M). The results showed that SO_4/SiO_2 acid catalyst treated with 2 M H_2SO_4 and calcined at 400 °C (SS-2-400) was the catalyst with highest total acidity (2.87 g/mmol), while the impregnation of Ni metal showed the highest acidity value at 3%/Ni-SS-2 catalyst (4.89 g/mmol). The SS-2-400 and 3%/Ni-SS-2 catalysts were selected and applied in the ethanol dehydration process into diethyl ether at temperatures 175, 200, and 225 °C. The activity and selectivity of SS-2-400 and 3%/Ni-SS-2 catalysts shown the conversion of ethanol reached up to 9.54% with good selectivity towards diethyl ether liquid product formation.

Keywords: sulfated silica; catalyst; nanoparticle; diethyl ether; fuel additives; ethanol

1. Introduction

The world's demand for energy originating from fossil fuels such as natural gas and petroleum oil continues to increase, while the availability of this fuel continues to decrease. The development of alternative fuels is one solution to reducing this [1,2]. Biofuels are environmentally friendly and renewable alternative energy sources to overcome this problem. Diethyl ether is one of the biofuels that can effectively be used as a fuel [3] due to its high octane and cetane numbers, with values of 110 and 125, respectively [4–7]. Its good combustion characteristics indicate that it can improve engine performance and reduce

fuel consumption [8]. Diethyl ether (DEE) is generally made by dehydrating ethanol compounds (Barbet process) with a homogeneous catalyst such as H_2SO_4. The conversion of ethanol into diethyl ether using an H_2SO_4 catalyst reached 23% DEE [9]. However, the drawback of this process is that it is expensive, corrosive, and the separation of catalyst and products at the end of the reaction is still difficult due to the homogeneous catalyst and DEE liquid product being mixed together. A solid acid catalyst is a heterogeneous catalyst and it was already been reported to overcome this problem in ethanol dehydration [10].

Silica as a catalyst matrix has high surface area, good chemical and thermal stability, uniform pore size, high adsorption capacity, and good pore framework for free diffusion between substrates [11,12]. As an inert material, the addition of sulfate ions (SO_4^{2-}) to the silica can improve its catalytic activities by increasing the acidity, surface area, thermal stability, and porosity [13,14]. The sulfate ions (SO_4^{2-}) act as ligands that donate a lone pair electron through the Oxygen atom and form a coordination bond with the Si^{4+} cation [15]. The addition of sulfate anions to silica (SO_4/SiO_2) will create Brønsted and Lewis acid sites from the sulfate group, which increases its catalytic activity in ethanol dehydration. Feng et al. [16] reported the catalytic activity of $Ti(SO_4)_2$/CS (Sulfated titania/activated carbon sphere) with catalyst for methanol dehydration into dimethyl ether (DME). $Ti(SO_4)_2$/CS catalyst reveal the conversion and selectivity of DME up to 11.7 and 75.8%, respectively. The high conversion of DME is due to the presence of weak acid and redox sites on the $Ti(SO_4)_2$/CS catalyst, which is suitable for direct oxidation of dimethyl ether.

Increasing the catalytic activity of SiO_2 catalyst has been widely investigated by the addition of metals. Platinum (Pt) and Palladium (Pd) noble metals are commonly used as dopants for SiO_2 supported catalyst fabrication. Supported Pt and Pd metal catalyst shows higher catalytic activity. However, these metals are less economical due to their high cost and limited availability. Pt and Pd metals are starting to be switched with non-noble transition metal that has low cost and is more available, such as Nickel (Ni) [17]. The catalytic activity of Nickel (Ni) as a support catalyst shows its good activity and acidity. Dehydration of ethanol to diethyl ether using Nickel (Ni) as a support catalyst has shown good catalytic activity and reached a conversion of diethyl ether up to 30% [18,19]. Ni metal is a type of transition metal that can act as a carrier in the adsorption of reactants on the surface of the catalyst. Ni metal forms coordination covalent bonds which can facilitate the formation of intermediates on the surface of the catalyst. In addition, Nickel has an unpaired electron which is capable of forming Brønsted acid site by hydrogen (H_2) splitting and a Lewis acid site as an electron acceptor from vacant of orbital (4p) that can accept electron pairs from Lewis bases [20,21]. Recent reports reveal that the addition of Nickel to a SiO_2 catalyst supports and enhances the hydrocracking of vegetable oil due to the presence of Ni dopants in the supported catalyst [21].

This study focused on the development of porous sulphated SiO_2 as a catalyst for the dehydration of ethanol into diethyl ether. The influence of sulfation on SiO_2 (SO_4/SiO_2 catalyst) was determined by the acidity value of the optimum sulfate concentration and calcination temperature. The catalyst with the highest acidity value was then impregnated with Nickel metal as Ni-SO_4/SiO_2. Based on the highest acidity of the catalyst, SO_4/SiO_2 and Ni-SO_4/SiO_2 was applied to determine the catalyst efficiency in the dehydration reaction of ethanol into diethyl ether.

2. Results and Discussion

2.1. FTIR Analysis

The infrared spectra of the SO_4/SiO_2 catalysts from the variations in H_2SO_4 concentration are shown in Figure 1. The absorptions at the wave number 460 and 815 cm^{-1} show the bending and symmetrical stretching vibrations in the Si-O-Si groups. The broad absorption band at 3600–3000 cm^{-1} represents the stretching vibration of the -OH group from silanol groups (Si-OH) [21]. Meanwhile, the bending vibration of the -OH group of silanol originated from the water molecule as confirmed through absorption at 1600 cm^{-1}.

The absorption at 1100 cm^{-1} shows the asymmetric stretching vibrations of the Si-O-Si groups overlapping with the stretching vibration of the S-OH from the HSO_4^{-1} ion [22].

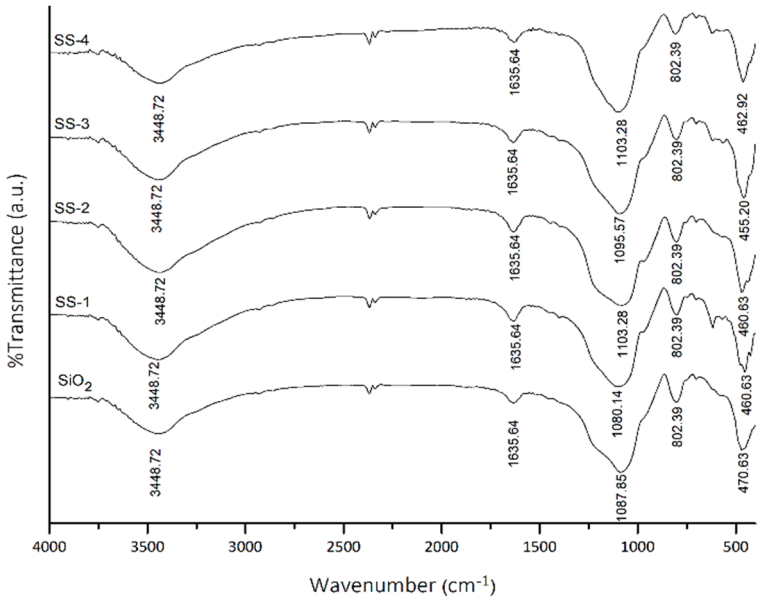

Figure 1. FTIR spectra of SiO_2, SS-1, SS-2, SS-3, and SS-4 catalyst. SS = Sulfated silica.

The spectra of the SO_4/SiO_2 catalysts show the less intense peak at 1467 and 1418 confirmed the presence of SO_4 symmetry and asymmetry stretching vibration, and indicated the sulfation was successfully carried out on silica framework [20,23]. The overlap of the absorption band at the wave number 1200–950 cm^{-1} for SiO_2 and SO_4^{2-} showed the shift to a smaller wavenumber due to the SO_4^{2-} ions was coordinated with the oxygen from SiO_2 [24,25].

The acidity test was carried out using the gravimetric method with pyridine gas. The acidity of SiO_2 and SO_4/SiO_2 catalysts at varying concentrations is shown in Table 1. SiO_2 has an acidity value of 2.08 mmol/g. The addition of sulfate to SiO_2 showed an increase in the acidity of catalysts. The SS-2-400 catalyst was shown to have the highest acidity (2.87 mmol/g), which was confirmed by the FTIR spectra of the SS-2 catalyst (Figure 1) that had the highest intensity of SO_4 vibration at 1467 and 1418 cm^{-1}. The acidity of the catalysts then decreased from SS-2-500 to SS-4-500. This can be attributed to the number and distribution of the sulfate groups on the surface that had reached a maximum value, causing the adsorbed pyridine molecules to decrease [26].

Table 1. Acidity values of SiO_2 and SO_4/SiO_2 catalysts.

Catalysts	Acidity (mmol/g)
SiO_2	2.08
SS-1	2.13
SS-2	2.22
SS-3	2.05
SS-4	1.68
SS-2-400	2.87
SS-2-500	2.22
SS-2-600	1.76

The SS-2 catalyst was then calcined at temperatures of 400, 500, and 600 °C. The FTIR spectra of SS-2 catalysts at various temperatures are shown in Figure 2. The influence of calcination temperature on the SS-2 catalysts caused the intensity of SO_4 vibrations (1467 and 1418 cm^{-1}) to decrease with increasing calcination temperature. The SS-2-400 catalyst showed the highest intensity of SO_4 vibrations. The acidity value of SS-2 catalysts (Table 1)

confirmed that the SS-2-400 catalyst has the highest acidity value (2.87 mmol/g). An increase in calcination temperature caused the acidity value of the catalysts to decrease due to the sulfate groups on the surface of the catalyst decomposing and releasing SO_3 [27,28].

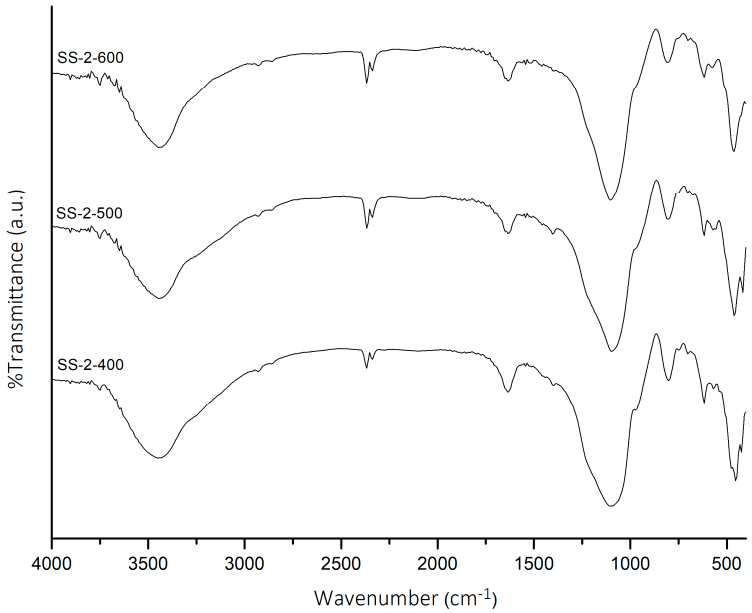

Figure 2. FTIR spectra of SS-2-400, SS-2-500, and SS-2-600.

2.2. XRD Analysis

The diffractograms of the SO_4/SiO_2 catalysts are shown in Figure 3. The wide peaks on the diffractograms indicate that the catalysts were amorphous [28]. The XRD patterns of each catalyst showed broad and large peaks at 2θ = 22° (101). The resulting two-theta angle, JCPDS 39-1425, indicated that the catalyst samples were naturally amorphous silica. The activation with sulfuric acid did not change the crystal structure of the silica material. The diffractogram of the silica treated with sulfate increased the intensities of silica caused by the sulfate ions that managed to enter the silica catalyst framework [29].

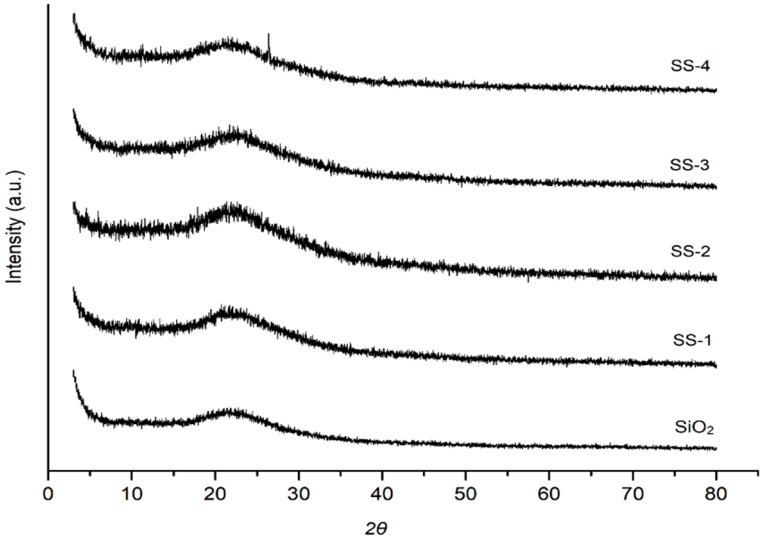

Figure 3. XRD diffraction of SiO_2, SS-1, SS-2, SS-3, and SS-4 catalyst. SS = Sulfated silica.

Figure 4 show an increased peak intensity of SiO_2 with the increase in calcination temperatures due to the aggregation of silica material and decomposition of sulfate groups at high temperature calcination [30]. The crystallite size was calculated using Scherrer equation. The increasing calcination temperature up to 600 °C influenced on the increasing of crystallite size 7.16, 11.9, and 14.7 nm for SS-2-400, SS-2-500, and SS-2-600, respectively. This condition was caused by the improvement of sulfate interaction with increasing calcination temperature up to 600 °C and the stability of the sulfate was broken due to overheating. The SS-2-400 catalyst has the highest sulfate groups, which gives it a broad peak, whereas the SS-2-500 and SS-2-600 catalysts show high peak intensity due to the increase in crystallinity catalysts with the decomposition of sulfate groups from the surface of catalysts.

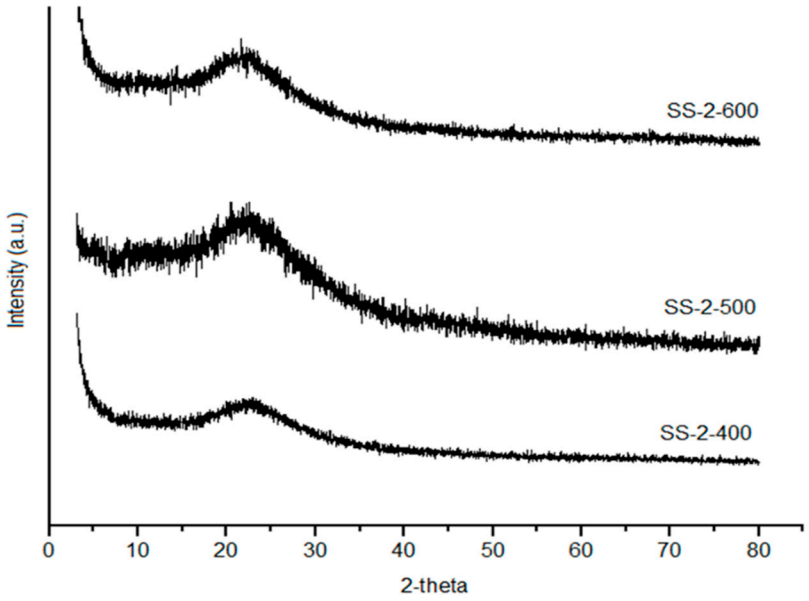

Figure 4. XRD diffraction of SS-2-400, SS-2-500, and SS-2-600.

2.3. Surface Morphology

The SEM images of SiO_2 and SO_4/SiO_2 catalysts are shown in Figure 5. The catalysts have an uneven sample surface consisting of chunks that form slabs with clear boundaries. The images present that the particle size of the samples was uneven, consequential of the amorphous character shown in the XRD characterization [31]. Based on the SEM images, the morphologies of SiO_2 and SS-2-400 catalysts demonstrated structural changes on the surface. The presence of sulfate caused the slabs on the SS-2-400 catalyst to have granules attached to them due to the presence of agglomeration [32]. Additionally, the SEM images of the SS-2-400 catalyst appeared brighter compared to SiO_2 due to the presence of highly charged sulfate ions [33]. Table 2 represents the EDS spectra of SiO_2 and SS-2-400 catalyst. The EDS spectra of SS-2-400 catalyst confirmed the presence of the element sulfur (0.97%) that indicated the sulfation was successfully carried out.

2.4. TGA/DSC Analysis

The TGA/DSC thermograms of SiO_2 and SS-2-400 catalysts are shown in Figure 6. The SiO_2 catalyst thermogram shows that the TGA curve had a mass reduction of 13.96% at temperatures of 0 to 165 °C, which indicated the release of water molecules from the catalyst. This is also reflected in the DSC curve at the temperature range of 34–169 °C, showing an endothermic peak due to the process of water molecule release. The wide endothermic peaks on the DSC curve in the temperature range of 400–1000 °C represent a mass reduction of 4.90%, which corresponds to vicinal silanol groups that are released from the SiO_2 [34]. The high mass reduction in this range implies that the sample was

dominated by water molecules that were bonded to silanol Si-OH and C-O [35]. The total change in mass of the SiO_2 catalyst at 0–1200 °C was 18.86%.

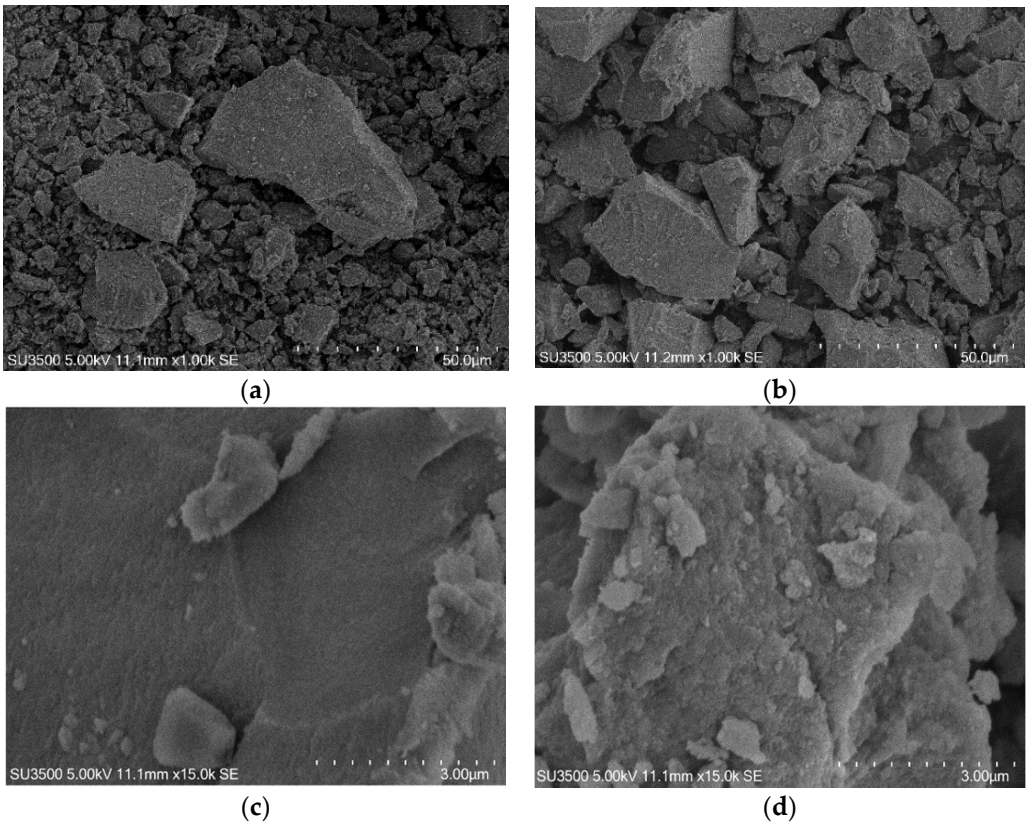

Figure 5. SEM images of SiO_2 (**a**,**c**) and SS-2-400 (**b**,**d**) catalysts at 1000× and 10.000× magnification.

Table 2. EDS SiO_2 and SS-2-400 catalyst.

Elements	Atom (%)	
	SiO_2	**SS-2-400**
Si	35.4	40.6
O	63.7	57.2
S	-	2.1

The thermogram of the SS-2-400 shows a mass decrease of 9.03% in the temperature range of 30–158 °C. The decrease in mass on the curve was a result of dehydration or loss of water molecules, as indicated by the presence of an endothermic peak on the DSC curve in the range of 0–150 °C. In the temperature range of 300–1200 °C, the TGA curve shows a mass reduction of 10.79% whilst the DSC curve shows high and wide endothermic peaks. The mass reduction that occurred denotes the SO_3 evolution process and the decomposition of sulfate ions that were attached to the SiO_2 catalyst [36]. The total reduction in mass of the SS-2-400 catalyst from 0–1200 °C was 23.86%.

2.5. Surface Area and Porosity Analysis

The surface and pore properties of SiO_2 and SS-2-400 catalysts are shown in Table 3. SiO_2 has a surface area of 772.15 (m^2/g). There was a decrease in surface area for the SS-2-400 catalyst (236.09 m^2/g), and the total pore volume of the catalyst due to the addition of sulfuric acid coating on the silica surface and the presence of agglomeration that covered the pores of the catalyst. The impregnation of sulfuric acid on SiO_2 caused a decrease in the pore volume of the catalyst due to the entry of sulfate groups into the silica surface.

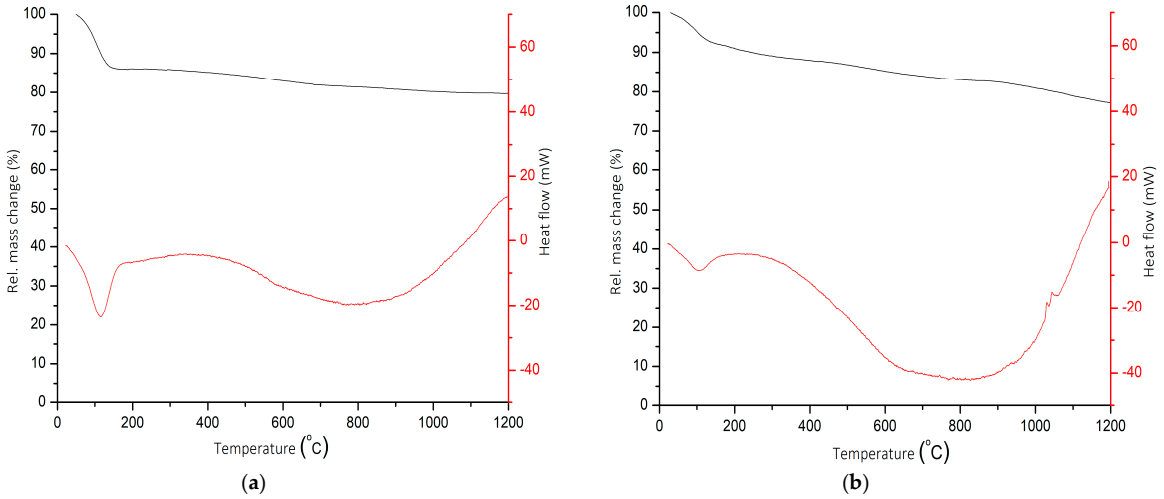

Figure 6. TGA/DSC thermograms of SiO_2 (**a**) and SS-2-400 (**b**) catalysts.

Table 3. Surface and pore properties of SiO_2 and SS-2-400 catalysts.

Catalyst	Surface Area (m^2/g)	Total Pore Volume (cc/g)	Pore Diameter (nm)
SiO_2	772.153	0.732	3.672
SS-2-400	236.093	0.407	6.624

The N_2 adsorption–desorption isotherm curves are shown in Figure 7. Based on IUPAC isotherm type, the SiO_2 and SS-2-400 catalysts have an isotherm type of IVa accompanied by a type H4 hysteresis loop, confirming that both catalysts are mesoporous materials. The H4 hysteresis loop also confirms the presence of a narrow slit-like pore and the filling of micropores [32].

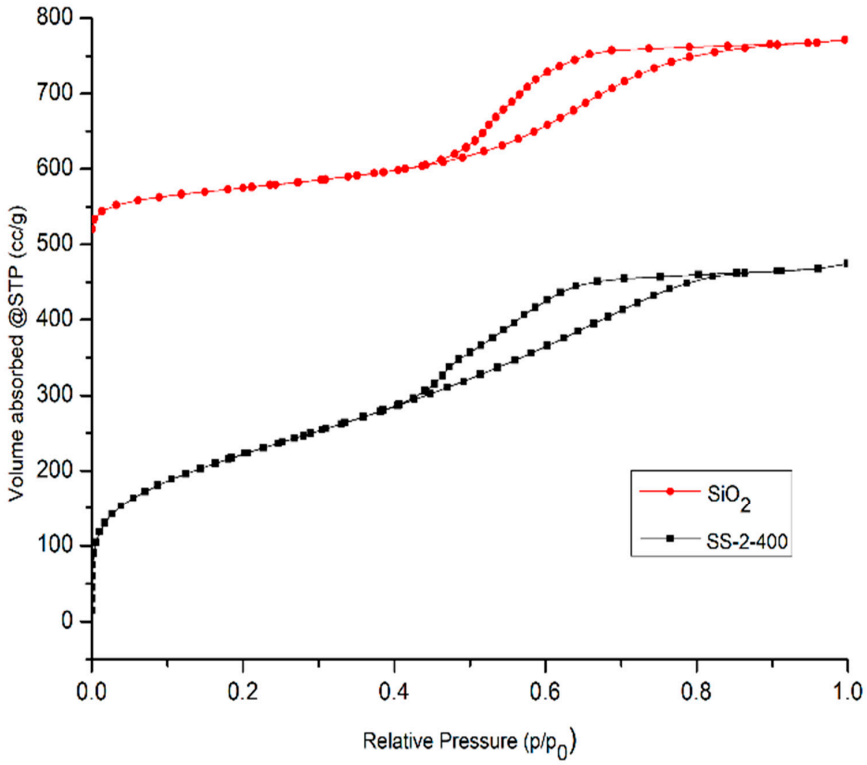

Figure 7. N_2 adsorption–desorption isotherms of SiO_2 and SS-2-400 catalysts.

SiO_2 and SO_4/SiO_2 catalysts also have micropore system characteristics obtained based on micropore analysis, which are shown in Table 4. The SiO_2 and SO_4/SiO_2 catalysts have pore diameters of 0.626 and 0.806 nm, respectively. It is indicated that the catalysts have a micropore structure with diameters of less than 2 nm and it is confirmed that the SiO_2 and SO_4/SiO_2 catalysts have micropore and mesoporous systems.

Table 4. Micropore analysis of SiO_2 and SO_4/SiO_2 catalysts.

Catalyst	Micropore Volume (cc/g)	Average Micropore Diameter (nm)
SiO_2	0.325	0.626
SS-2-400	0.407	0.806

2.6. Characterization of Ni-SO_4/SiO_2 Catalyst

The impregnation of nickel metal with concentration 1, 2 dan 3% to the SS-2-400 catalyst was successfully carried out. An Atomic Absorption Spectroscopy (AAS) instrument was used to determine the amount of Ni metal impregnated into the catalyst. The amount of Ni metal content of the Ni-SO_4/SiO_2 catalyst is shown in Table 5. The higher concentration of Ni metal that was impregnated shows an increase in the Ni metal content of the Ni-SO_4/SiO_2 catalyst. The 3%/Ni-SS-2-400 catalyst was the catalyst with the highest Ni metal content of 2.18%.

Table 5. Ni metal content of Ni-SO_4/SiO_2 catalyst.

Catalysts	Ni Metal Content (AAS/wt%)
1%/Ni-SS-2	0.74
2%/Ni-SS-2	1.55
3%/Ni-SS-2	2.18

The acidity value of the Ni-SO_4/SiO_2 catalyst was determined by a gravimetric method using ammonia adsorption, which is shown in Table 6. The impregnated nickel metal to the SS-2-400 catalyst raised the catalyst's acidity value. This is confirmed by the fact that Ni metal as a catalyst support on SiO_2 showed a good acidity value. Ni metal has an unpaired electron and electron acceptor which is capable of forming Brønsted and Lewis acids, which are the main acid sites of the catalyst [18,24,25]. The 3%/Ni-SS-2-400 catalyst with the highest Ni metal content also shows a higher acidity value (7.69 mmol/g). This indicates that Ni metal influences the acidity of the SO_4/SiO_2 catalyst. Nurmalasari et al. [37] reported the impregnated of Ni metal on mesoporous silica for hydrocracking of waste lubricant, stating that the presence of Ni metal increases the acidity value of silica from 5.1 to 7.1 mmol/g.

Table 6. Acidity values of Ni-SO_4/SiO_2 catalyst.

Catalysts	Acidity (mmol/g)
SS-2-400	2.87
1%/Ni-SS-2	5.16
2%/Ni-SS-2	6.38
3%/Ni-SS-2	7.69

Figure 8 shows the FTIR spectra of Ni-SO_4/SiO_2 catalyst after acidity test, which confirmed the presence of Brønsted and Lewis acids site on catalyst. A new absorption peak occurs in the wavenumber 1402 cm^{-1}, which confirms the Brønsted acid site from the -NH asymmetric stretching vibration, while at 1643 cm^{-1}, identified as Lewis acid sites from the coordinated symmetric bending vibration -NH, which is overlapping with the stretching vibration of the -OH group [38,39], the band at 798 cm^{-1} represents the stretching vibration of Ni from the Ni-SO_4/SiO_2 catalyst [18].

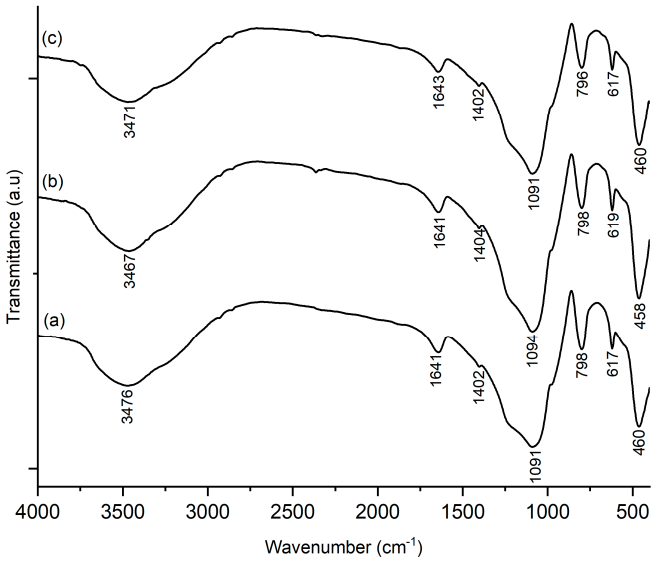

Figure 8. FTIR spectra acid tested of (**a**) 1%/Ni-SS-2; (**b**) 2%/Ni-SS-2; (**c**) 3%/Ni-SS-2.

2.7. Study of Activity and Selectivity of SiO_2, SO_4/SiO_2 and Ni-SO_4/SiO_2 Catalysts

The activity and selectivity of the catalysts were tested by dehydrating ethanol into diethyl ether. The catalytic activity was evaluated as the percentage of total conversion and the liquid yield of DEE with the various temperatures of 175, 200, and 225 °C. The amount of liquid product conversion was used to determine the selectivity of the catalyst. DEE was determined using the spiking method. The spiking method was performed by comparing the peak intensity before and after adding the standard. Intensity will increase if the same compound is added to the standard compound and the compound being analyzed. The catalyst that was applied for the activity and selectivity tests was the SS-2-400 catalyst as the catalyst with the highest acidity value, as well as the SiO_2 catalyst as a comparison.

The conversion activity and selectivity in the ethanol dehydration reaction of the SS-2-400 catalyst (Figure 9) tended to be higher than that of the SiO_2 catalyst. This is due to the addition of sulfate ions onto the silica catalyst, which can increase the number of Brønsted and Lewis acid sites—a major factor in the successful performance of the catalyst. The selectivity of the SS-2-400 catalyst in the conversion of ethanol into diethyl ether increased with the increased in reaction temperatures [10]. The liquid product of each catalyst showed the highest conversion at a temperature of 225 °C of 45.3 and 66.75%, respectively. The selectivity of the SiO_2 catalyst at the temperatures of 175 and 200 °C was not able to produce diethyl ether as the DEE content was 0%. However, the catalytic reaction at the temperature of 225 °C with the SiO_2 catalyst resulted in a DEE content of 1.93%. The difference in these results indicates that reaction temperature plays an important role in the ethanol dehydration process, and the dehydration of ethanol into diethyl ether using SiO_2 catalyst must be carried out at a temperature of over 200 °C. The SS-2-400 catalyst has good selectivity in the DEE conversion and reaches the conversion of DEE up to 9.54% at a temperature of reaction of 225 °C.

The catalytic activities of the catalysts produced from the SS-2-400 catalyst impregnated with Ni metal were also examined. The results of the catalyst selectivity test based on the conversion of diethyl ether can be seen in Figure 10. The diethyl ether conversion was generally much better after the impregnation of the Ni metal. The higher the Ni metal concentration, the higher the DEE produced. This is influenced by the acidity and catalytic activity of the catalyst in the presence of Ni metal, which provide empty orbitals that increase the number of Brønsted and Lewis acid sites in the catalyst [40]. The 3%/Ni-SS-2 catalyst showed the highest conversion of liquid and DEE conversion: 84.03 and 24.01%, respectively. This is in accordance with the acidity value data, in which the 3%/Ni-SS-2 catalyst had the highest acidity, indicating that the acidity of the catalyst influences the DEE yield.

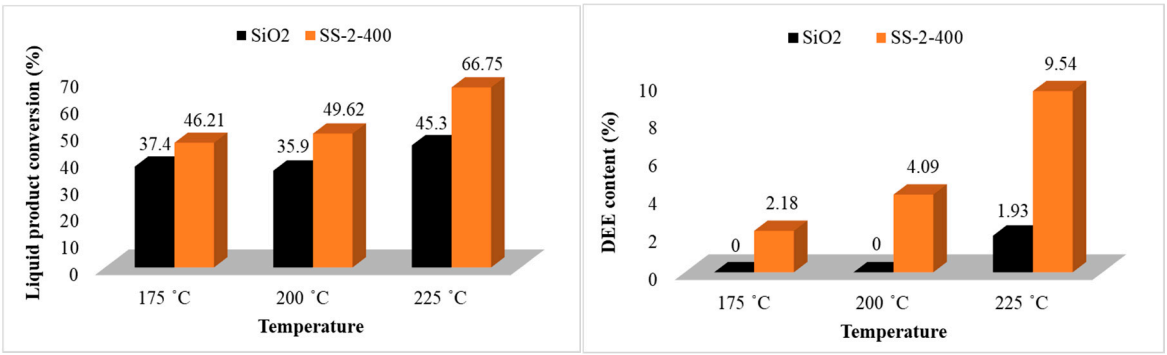

(**a**) (**b**)

Figure 9. Graphs of catalyst (**a**) activity and (**b**) selectivity of SiO_2 and SS-2-400 catalysts.

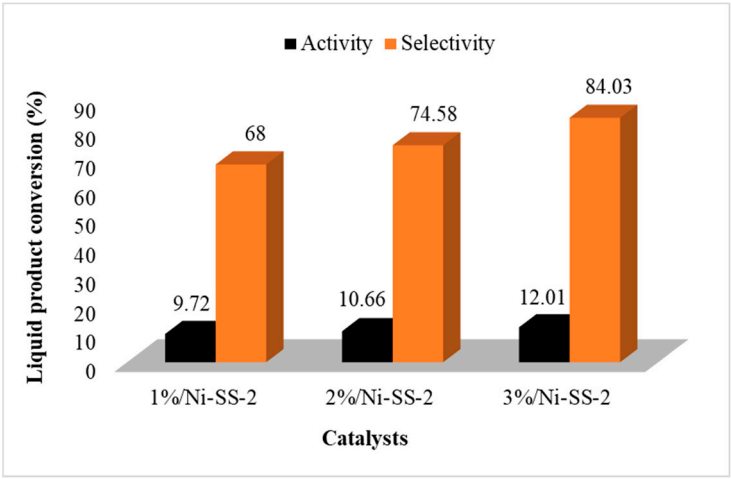

Figure 10. Graph of the activity (conversion) and selectivity of Ni-SO_4/SiO_2 catalysts.

The illustration of non-porous silica catalyst, porous silica catalyst, and surface of sulfated silica catalyst are shown in Figure 11. Porous silica catalyst Figure 11b, which was treated with the addition of $NaHCO_3$, had a larger surface area and pore size than non-porous silica (a). Figure 11c shown the condition of active sites on the surface of sulfated silica catalyst for DEE conversion. The factors that influence the results of the ethanol dehydration process are the surface area and pore size of the heterogeneous catalyst. The molecular size of diethyl ether simulated on HyperChem with the ab initio computational method is 6.67 Å or 0.667 nm. Therefore, to maximize the effectivity of the dehydration reaction on the surface of the catalyst, a pore system with a size that corresponds to the molecular size of diethyl ether is required.

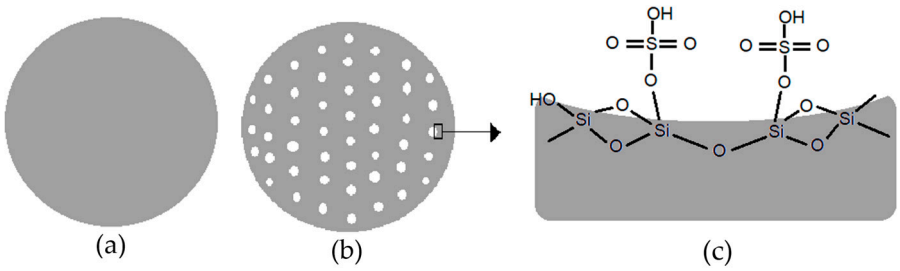

Figure 11. Illustration of (**a**) non-porous silica catalyst; (**b**) porous silica catalyst, and (**c**) surface of sulfated silica catalyst.

The SO_4/SiO_2 catalyst had higher surface area of 236.09 m^2/g, pore diameter of 6.624 nm (mesoporous system), and micropore diameter of 0.806 nm (micropore system). The pore diameters of the SO_4/SiO_2 catalyst found are relatively in accordance with the size of the diethyl ether molecule, thus allowing the dehydration reaction to work effectively and produce higher DEE levels.

3. Experimental

3.1. Materials

The materials used in this study were ethanol (C_2H_5OH; 96%), tetraethyl orthosilicate (TEOS), methanol (CH_3OH), hydrochloric acid (HCl; 37%), sulfuric acid (H_2SO_4; 98%), pyridine (C_5H_5N), ammonia (NH_3), nickel chloride hexahydrate ($NiCl_2 \cdot 6H_2O$), nitrogen gas, and sodium bicarbonate ($NaHCO_3$; 99%), all of them obtained from Merck.

3.2. SO_4/SiO_2 Catalyst Preparation

A total of 16.8 mL TEOS, 30 mL ethanol, and 10 mL H_2SO_4 (with concentrations of 1, 2, 3 M) were mixed and then stirred to form a gel. The gel was heated in an oven for 3 h at 100 °C and refluxed with methanol for 72 h. The solid was separated by centrifugation for 20 min at 2000 rpm and dried at 80 °C. The solids produced were calcined at 500 °C and labeled as SS-1-500, SS-2-500, and SS-3-500, later tested for their acidity. The catalyst with the highest acidity was calcined at temperatures of 400, 500, and 600 °C and then labeled as SS-x-400, SS-x-500, and SS-x-600. Each catalyst was characterized using FTIR and XRD. This was followed, again, with an acidity test. The catalyst with the highest acidity was then characterized using SEM, SAA, and TGA/DSC.

3.3. Ni-SO_4/SiO_2 Catalyst Preparation

The catalyst with the highest acidity was then impregnated with Nickel metal with concentrations of 1, 2, and 3%. Impregnation was achieved by stirring for 24 h at room temperature. The solid was separated by centrifugation at 2000 rpm and dried in an oven at 100 °C before being calcined at 500 °C for 4 h. The Ni-SS-2 catalysts were labeled as 1%/Ni-SS-2, 2%/Ni-SS-2, and 3%/Ni-SS-2 and tested for their acidity value and characterized using acidity test, FTIR, and AAS.

3.4. Ethanol Dehydration into Diethyl Ether

The catalytic activity of the SiO_2, SO_4/SiO_2 and Ni-SO_4/SiO_2 catalysts for the dehydration of ethanol to diethyl ether was tested in a reactor furnace system batch equipped with temperature and pressure controllers. A total of 20 mL of ethanol and catalyst (2 wt%) were fed into reactor in a different batch and flowed the N2 gas. The catalytic activity and selectivity were carried out at temperatures of 175, 200, and 225 °C with constant liquid hourly space velocity (LHSV). The DEE product was then characterized using GCMS analysis.

3.5. Characterization

Catalyst characterization was carried out using Fourier Transform InfraRed (FTIR) spectroscopy using Shimadzu Prestige-21 (Tokyo, Japan) with a wave number range of 4000–400 cm^{-1} and the KBr pellet technique. X-ray Diffraction (XRD) analysis was performed using the X'pert Pro PANalytical (Morgan Hill, CA, USA) with a Cu X-ray tube (1.5406 Å). The acidity test was carried out gravimetrically using pyridine vapor. Scanning Electron Microscope (SEM) imaging and elemental analysis were performed using High-Tech's scanning electron microscope (Hitachi) SU 3500 (Tokyo, Japan). Surface area analyzer (SAA) was performed using Quantachrome Quadrasorb-Evo Surface Area and Pore (London, UK). Size Analyzer Thermogravimetry analysis and Differential Scanning Calorimeter (TGA/DSC) were carried out in a free atmosphere with a temperature range of 30–1200 °C (temperature increase rate of 10 °C/minute). Atomic Absorption Spectrometer (AAS) was carried out using Perkin Elmer, 5100 PC (Tokyo, Japan); analysis of the liquid

products used Gas Chromatography (GC) GC 148 Shimadzu (FID) (Tokyo, Japan) with HP5 chromatography column (5% Phenyl Methyl Siloxane).

4. Conclusions

The effects of sulfation at various concentration and calcination temperatures on the preparation of sulfated silica catalyst have been studied. The SS-2-400 catalyst was found to have the optimum sulfate concentration and calcination temperature conditions shown by the acidity value of 2.87 mmol/g pyridine, which was highest among the sulfated silica catalyst. The sulfated silica catalyst had mesoporous and micropore systems with pore diameters of 6.624 and 0.806 nm, respectively. The pore size that sufficiently matched the diameter of the diethyl ether molecule allowed the dehydration process to occur more effectively. The highest yield from the ethanol dehydration reaction was obtained using the SS-2-400 catalyst at a temperature of 225 °C at 9.54%. Impregnation of Ni metal on the SS-2-400 catalyst found the optimum Ni metal and acidity value of 3%/Ni-SS-2 catalyst of 2.18 wt% and 7.68 mmol/g. The activity and selectivity of 3%/Ni-SS-2 catalyst show the highest conversion of liquid and DEE conversion at 84.03 and 24.01%, respectively.

Author Contributions: Conceptualization, K.W.; methodology, K.W. and M.U.; software, A.P.; validation, A.P.; formal analysis, M.L.L.M.; investigation, M.L.L.M.; resources, S.M.; data curation, A.C.W.; writing—original draft preparation, K.W.; writing—review and editing, J.R.R. and M.C.; visualization, J.R.R.; supervision, K.W.; project administration, K.W.; funding acquisition, H.A.A.-L. All authors have read and agreed to the published version of the manuscript.

Funding: Funding financial support by the Researchers Supporting Project Number (RSP-2021/54).

Acknowledgments: The authors express thanks for financial support by the Researchers Supporting Project Number (RSP-2021/54) King Saud University, Riyadh, Saudi Arabia. The work was supported by RISET KOLABORASI INDONESIA (RKI) 2020, Number: 356813/UN1/DITLIT/DITLIT/PT/2020.

Conflicts of Interest: The authors declare no conflict of interest.

References

1. Abidin, S.Z.; Haigh, K.F.; Saha, B. Esterification of free fatty acids in used cooking oil using ion-exchange resins as catalysts: An efficient pretreatment method for biodiesel feedstock. *Ind. Eng. Chem. Res.* **2012**, *51*, 14653–14664. [CrossRef]
2. Huang, D.; Zhou, H.; Lin, L. Biodiesel: An alternative to conventional fuel. *Energy Procedia* **2012**, *16*, 1874–1885. [CrossRef]
3. Kapasi, Z.A.; Nair, A.R.; Somawane, S. Biofuel an alternative source of energy for presence and future. *J. Adv. Sci. Technol.* **2010**, *13*, 105–108.
4. Alharbi, W.; Brown, E.; Kozhevnikova, E.F.; Kozhevnikov, I.V. Dehydration of ethanol over heteropoly acid catalysts in the gas phase. *J. Catal.* **2014**, *319*, 174–181. [CrossRef]
5. Rahmanian, A.; Ghaziaskar, H.S. Continuous dehydration of ethanol to diethyl ether over aluminum phosphate-hydroxyapatite catalyst under sub and supercritical condition. *J. Supercrit. Fluids* **2013**, *78*, 34–41. [CrossRef]
6. Varisli, D.; Dogu, T.D.G. Ethylene and diethyl-ether production by dehydration reaction of ethanol over different heteropolyacid catalysts. *Chem. Eng. Sci.* **2007**, *62*, 5349–5352. [CrossRef]
7. Takahara, I.; Saito, M.; Inaba, M.; Murata, K. Dehydration of ethanol into ethylene over solid acid catalysts. *Catal. Lett.* **2005**, *105*, 249–252. [CrossRef]
8. Ibrahim, A. Investigating the Effect of using diethyl ether as a fuel additive on diesel engine performance and combustion. *Appl. Therm. Eng.* **2016**, *107*, 853–862. [CrossRef]
9. Al-Faze, R.; Kozhevnikova, E.F.; Kozhevnikov, I.V. Diethyl ether conversion to ethene and ethanol catalyzed by heteropoly acids. *ACS Omega* **2021**, *6*, 9310–9318. [CrossRef] [PubMed]
10. Winata, W.F.; Wijaya, K.; Mara, A.; Kurniawati, W. Conversion of bioethanol to diethyl ether catalyzed by sulfuric acid and zeolite. *J. Idn. Chem. Soc.* **2020**, *3*, 151–157. [CrossRef]
11. Bergna, H.E.; Roberts, W.O. Colloidal silica: Fundamentals and applications, in Surfactant Science Series. *Mech. Eng. J.* **2006**, *22*, 9–37.
12. Fricke, J.; Emmerling, A. Aerogels, preparation, properties, applications. In *Structure and Bonding 77: Chemistry, Spectroscopy and Applications of Sol-Gel Glasses*; Springer: Berlin/Heidelberg, Germany, 1992.
13. Lion, M.; Maache, M.; Lavalley, J.C.; Ramis, G.; Busca, G.; Rossi, P.F.; Lorenzelli, V. FT-IR study of the brønsted acidity of phosphated and sulphated silica catalysts. *J. Mol. Struct.* **1990**, *218*, 417–422. [CrossRef]

14. Zhuang, Q.; Miller, J.M. One-pot sol-gel synthesis of sulfated ZrO_2-SiO_2 catalysts for alcohol dehydration. *Can. J. Chem.* **2001**, *79*, 1220–1223. [CrossRef]
15. Fu, B.; Gao, L.; Niu, L.; Wei, R.; Xiao, G. Biodiesel from waste cooking oil via heterogeneous superacid catalyst SO_4^{2-}/ZrO_2. *Energy Fuels* **2009**, *23*, 569–572. [CrossRef]
16. Feng, R.; Gao, X.J.; Yang, Q.; Li, M.J.; Zhang, J.F.; Song, F.; Zhang, Q.D.; Han, Y.Z.; Tan, Y.S. Effects of calcination temperature on the catalytic performance of $Ti(SO_4)_2$/CS for DME direct oxidation to polyoxymethylene dimethyl ethers. *J. Fuel Chem. Technol.* **2021**, *49*, 72–79. [CrossRef]
17. Nikolic, V.M.; Zugic, D.L.; Perovic, I.M.; Saponjic, A.B.; Babic, B.M.; Pasti, I.A.; Kaninski, M.P.M. Investigation of tungsten carbide supported Pd or Pt as anode catalysts for PEM fuel cells. *Int. J. Hydrogen Energy* **2013**, *38*, 11340–11345. [CrossRef]
18. Zhang, Y.; Liu, Q. Nickel phyllosilicate derived Ni/SiO_2 catalysts for CO_2 methanation: Identifying effect of silanol group concentration. *J. CO_2 Util.* **2021**, *50*, 101587. [CrossRef]
19. Susi, E.P.; Wijaya, K.; Pratika, R.A.; Hariani, P.L. Effect of nickel concentration in natural zeolite as catalyst in hydrocracking process of used cooking oil. *Asian J. Chem.* **2020**, *32*, 2773–2777. [CrossRef]
20. Sarve, D.T.; Singh, S.K.; Ekhe, J.D. Kinetic and mechanistic study of ethanol dehydration to diethyl ether over Ni-ZSM-5 in a closed batch reactor. *React. Kinet. Mech. Catal.* **2020**, *131*, 261–281. [CrossRef]
21. Wijaya, K.; Syoufian, A.; Ariantika, S. Hydrocracking of used cooking oil into biofuel catalyzed by nickel-bentonite. *Asian J. Chem.* **2014**, *26*, 6097–6100. [CrossRef]
22. Radwan, N.R.E.; Hagar, M.; Afifi, T.H.; Al-wadaani, F.; Okasha, R.M. Catalytic activity of sulfated and phosphated catalysts towards the synthesis of substituted coumarin. *Catalysts* **2018**, *8*, 36. [CrossRef]
23. Yang, Z.W.; Niu, L.Y.; Jia, X.J.; Kang, Q.X.; Ma, Z.H.; Lei, Z.Q. Preparation of silica-supported sulfate and its application as a stable and highly active solid acid catalyst. *Catal. Commun.* **2011**, *12*, 798–802. [CrossRef]
24. Du, Y.; Sun, Y.; Di, Y.; Zhao, L.; Liu, S.; Xiao, S.F. Ordered mesoporous sulfated silica-zirconia materials with high zirconium contents in the structure. *J. Porous. Mater.* **2006**, *13*, 163–171. [CrossRef]
25. Sunajadevi, K.R.; Sugunan, S. Synthesis, Characterization and benzylation activity of nanocrystalline chromia loaded sulfated titania prepared via sol-gel route. *Catal. Commun.* **2004**, *5*, 575–581. [CrossRef]
26. Ahmed, A.I.; El-Hakam, S.A.; Samra, S.E.; L-Khouly, A.A.E.; Khder, A.S. Structural characterization of sulfated zirconia and their catalytic activity in dehydration of ethanol. *Colloids Surf. A Physicochem. Eng. Asp.* **2008**, *317*, 62–70. [CrossRef]
27. Pratika, R.A.; Wijaya, K.; Trisunaryanti, W. Hydrothermal treatment of SO_4/TiO_2 and TiO_2/CaO as heterogeneous catalysts for the conversion of Jatropha oil into biodiesel. *J. Environ. Chem. Eng.* **2021**, *9*, 106547. [CrossRef]
28. Hanafi, M.F.; Sapawe, N. Effect of calcination temperature on the structure and catalytic performance of ZrO_2 catalyst in phenol degradation. *Mater. Today Proc.* **2019**, *19*, 1533–1536. [CrossRef]
29. Wijaya, K.; Saputri, W.D.; Aziz, I.T.A.; Heraldy, E.; Hakim, L.; Suseno, A.; Utami, M. Mesoporous silica preparation using sodium bicarbonate as template and application of the silica for hydrocracking of used cooking oil into biofuel. *Silicon* **2021**, *13*, 1–9. [CrossRef]
30. Aneu, A.; Wijaya, K.; Syoufian, A. Silica-based solid acid catalyst with different concentration of H_2SO_4 and calcination temperature: Preparation and characterization. *Silicon* **2020**, *13*, 2265–2270. [CrossRef]
31. Patel, A.; Brahmkhatri, V.; Singh, N. Biodiesel production by esterification of free fattyacid over sulfated zirconia. *Renew. Energy* **2013**, *51*, 227–233. [CrossRef]
32. Utami, M.; Trisunaryanti, W.; Shida, K.; Tsushida, M.; Kawakita, H.; Ohto, K.; Wijaya, K.; Tominaga, M. Hydrothermal preparation of a platinum-loaded sulphated nanozirconia catalyst for the effective conversion of waste low density polyethylene into gasoline-range hydrocarbons. *RSC Adv.* **2019**, *9*, 41392. [CrossRef]
33. Aboul-Gheit, A.K.; Gad, F.K.; Abdel-Aleem, G.M.; El-Desouki, D.S.; Abdel-Hamid, S.M.; Ghoneim, S.A.; Ibrahim, A.H. Pt, Re and incorporation in sulfated zirconia as catalyst for n-pentane isomerization. *Egypt. Pet.* **2014**, *23*, 303–314. [CrossRef]
34. Charmas, B.; Kucio, K.; Sydorchuk, V.; Khalameida, S.; Zięzio, M.; Nowicka, A. Characterization of multimodal silicas using TG/DTG/DTA, Q-TG, and DSC methods. *Colloids Interfaces* **2018**, *3*, 6. [CrossRef]
35. Thommes, M.; Kaneko, K.; Neimark, A.V.; Olivier, J.P.; Rodriguez-Reinoso, F.; Rouquerol, J.; Sing, K.S. Physisorption of gases, with special reference to the evaluation of surface area and pore size distribution. *Pure Appl. Chem.* **2015**, *87*, 1051–1069. [CrossRef]
36. Yang, X.; Guo, S. Pore characterization of marine-continental transitional shale in permian shanxi formation of the southern north china basin. *Energy Explor. Exploit.* **2020**, *38*, 2199–2216. [CrossRef]
37. Nurmalasari, W.T.; Sutarno, I.I.F. Mesoporous silica impregnated by Ni and NiMo as catalysts for hydrocracking of waste lubricant. *Int. J. ChemTech Res.* **2016**, *9*, 607–614. [CrossRef]
38. Niwa, M.; Nishinikawa, S.; Katada, N. IRMS–TPD of ammonia for characterization of acid site in b-zeolite. *Microporous Mesoporous Mater.* **2005**, *82*, 105–112. [CrossRef]
39. Wijaya, K.; Kurniawan, M.A.; Saputri, W.D.; Trisunaryanti, W.; Mirzan, M.; Hariani, P.L.; Tikoalu, A.D. Synthesis of nickel catalyst supported on ZrO_2/SO_4 pillared bentonite and its application for conversion of coconut oil into gasoline via hydrocracking process. *J. Environ. Chem. Eng.* **2021**, *9*, 105399. [CrossRef]
40. Amin, K.A.; Wijaya, K.; Trisunaryanti, W. The catalytic performance of ZrO_2-SO_4 and Ni/ZrO_2-SO_4 prepared from commercial ZrO_2 in Hydrocracking of LDPE plastic waste into liquid fuels. *Orient. J. Chem.* **2018**, *34*, 3070. [CrossRef]